J. Cent. South Univ. (2022) 29: 2084−2098
DOI: https://doi.org/10.1007/s11771-022-5065-y

Springer

Valorization of natural diatomite mineral: Application to removal of anionic dye from aqueous solution in a batch and fixed-bed reactor

HADRI Mohamed[1, 2], EL MRABET Imane[1], CHAOUKI Zineb[1], DRAOUI Khalid[2], HAMDAOUI Mustapha[2], DOUHRI Hikmat[2], ZAITAN Hicham[1]*

1. Processes, Materials, Environment Laboratory (LPME), Faculty of Sciences and Technology, Sidi Mohamed Ben Abdellah University, B.P. 2202, Fez, Morocco;
2. Laboratory MSI, Faculty of Sciences, Abdel Malek Essaadi University, B.P. 2121, M'hannech II, 93002, Tetouan, Morocco

Abstract: In this work, the efficiency of an adsorption process, in which Moroccan diatomite (ND) is used as a low-cost adsorbent to remove Congo red (CR) dye from contaminated waters in batch and column system, was examined. The influence of experimental conditions (pH, adsorbent dose and temperature) on the adsorption of CR onto the ND adsorbent was studied. A study of the adsorption kinetics for CR revealed that a pseudo-second-order model provided the best fit to the experimental kinetic data, and the equilibrium data were well described by the Langmuir isotherm model with an adsorption capacity of 6.07 mg/g using 15 g/L of ND, pH=6, contact time 3 h and 25 °C. On the other hand, the ND regeneration tests were investigated and showed that the desorption reaches at least 50% when using ethanol as eluent. In addition, the adsorption process in a continuous mode was studied. Breakthrough curves were properly represented by the Yoon−Nelson model. Hence, the adsorption capacity of 5.71 mg/g was reached using 0.114 g of adsorbent, CR concentration of 6 mg/L and a flow of 1 mL/min under 25 °C.

Key words: Congo red; adsorption; diatomite; fixed-bed column; kinetic model

Cite this article as: HADRI Mohamed, EL MRABET Imane, CHAOUKI Zineb, DRAOUI Khalid, HAMDAOUI Mustapha, DOUHRI Hikmat, ZAITAN Hicham. Valorization of natural diatomite mineral: Application to removal of anionic dye from aqueous solution in a batch and fixed-bed reactor [J]. Journal of Central South University, 2022, 29(6): 2084−2098. DOI: https://doi.org/10.1007/s11771-022-5065-y.

1 Introduction

The scarcity of water resources and degradation of their quality have become a major environmental challenge all over the world and Morocco is no exception [1−5]. In this regard and with the aim of ensuring the preservation of water resources, Morocco has turned towards non-conventional water resources, in particular the desalination of seawater, the reuse of purified effluents (industrial and/or agricultural) and rainwater collection. Therefore, considerable efforts have been made in Morocco during the last decades in the wastewater treatment sector [6−9].

Various physicochemical and biological methods have been developed to remove dyes from wastewaters, varying in process effectiveness, operation and costs. On the basis of these conditions, the adsorption process is the most popular treatment method for the removal of dyes from aqueous conditions due to its simplicity, ease

Received date: 2021-02-13; **Accepted date:** 2021-08-09
Corresponding author: ZAITAN Hicham, PhD, Professor; E-mail: hicham.zaitan@usmba.ac.ma; ORCID: https://orcid.org/0000-0002-2542-3240

of adsorbent recovery and low cost compared with other treatment processes.

The long-standing use of activated carbon as an adsorbent seems to be effective in the removal of dye contaminants from wastewaters. However, it is proved to be fraught with several problems such as the high operating cost and difficulty of regeneration for reuse, which limits the possibility of using it [10]. Hence, finding alternative natural adsorbents that are both inexpensive and effective for industrial application is becoming increasingly important. In this context, adsorption onto mineral materials has gained the interest of many researchers in recent years.

In a recent study, the Moroccan diatomite adsorbent was used in the adsorption of organic pollutants in aqueous solutions with a high adsorption efficiency for methylene blue dye [11]. Indeed, the diatomite is considered a strong candidate for use as an adsorbent to remove the anionic dye from wastewaters due to its availability and low cost.

Cationic dyes have been examined extensively, but anionic dyes have received little attention, which is why we have chosen the Congo red. It is used in this study as a target organic pollutant and representative of environmental relevance anionic dyes. Congo red is an anionic azo dye used in histology in many staining formulations, and as a dye for textiles (wool and silk), paper, leather, wood stain [12] and is generally resistant to biodegradation due to its xenobiotic nature [13] which poses serious and deleterious effects on the environment, human health and aquatic life when released untreated [14].

On the other hand, the adsorption process is usually restricted to experiments in batch mode, which is useful to elucidate adsorption capacities parameters for dye removal although its lack of applicability when scaling up is being considered for real wastewater treatment systems [15−16].

For this purpose, research in a continuous flow using a small-scale fixed-bed column is more suitable for predicting the adsorption performance of the investigated diatomite.

In this framework, the aim of the current work is to evaluate the potential use of Moroccan natural diatomite (ND) as a low-cost adsorbent for the removal of a representative acidic dye (CR) from aqueous solutions. Hence, the ND was tested in batch and continuous modes. The effects of various operational parameters (diatomite dose, initial dye concentration, contact time, temperature and the initial pH of the solution) were investigated. Different adsorption isotherms and kinetic models were used to assess the equilibrium data and to provide a better understanding of adsorption process characteristics and removal efficiencies. The degree of adsorption capacity recovery after various cycles of adsorption onto ND followed by desorption with various desorbing agents was also assessed. Finally, continuous removal of the CR was assessed from experiments in an up-flow column.

2 Materials and methods

2.1 Materials

Natural diatomite (ND) was obtained from the Nador area (Morocco). The material was used without any previous activation. The ND samples were firstly crushed, washed with distilled water several times. After washing, it was dried at 110 °C in an oven for 24 h and was finally ground into powders (~60 μm). The resulting powders were stored in hermetic glass bottles for future use.

The physico-chemical and morphological properties of the ND have been studied in detail by HADRI et al [11], where the key physical-chemical properties of ND are reported in Table 1. Hence, these characteristics may provide interactions between the CR and the ND particles which could enhance significantly the adsorption performance.

Table 1 Physical-chemical properties of ND

S_{BET}[a]	V_t[b]	V_{meso}[c]	V_{micro}[d]	D_p[e]	pH_{PZC}[f]	TAS[g]
17.36	0.06	0.04	0.02	1.94	6.5	2.65

TBS[h]	TS[i]	$w(SiO_2)$/%	$w(Al_2O_3)$/%	w(CaO)/%	$w(Fe_2O_3)$/%
0.43	3.08	72.8	5.22	5.86	1.94

[a] Specific surface area ($m^2 \cdot g^{-1}$); [b] Total pore volume ($cm^3 \cdot g^{-1}$); [c] Mesoporous volume ($cm^3 \cdot g^{-1}$); [d] Microporous volume ($cm^3 \cdot g^{-1}$); [e] Pore diameter (nm); [f] pH of the point of zero charge; [g] Total acidic sites ($mmol \cdot g^{-1}$); [h] Total basic sites ($mmol \cdot g^{-1}$); [i] Total sites ($mmol \cdot g^{-1}$).

The Congo red (CR) was supplied by HiMedia (HiMedia Laboratories, Mumbai, India). All of the chemicals used in the study were purchased from Sigma-Aldrich (Sigma-Aldrich Chimie S. A. R. L., Lyon, France) as reagent grade and were used without further purification.

2.2 Batch adsorption−desorption

CR adsorption experiments were carried out using the batch method. A mass of 20 mg of ND was added in 20 mL solution of CR solution at pH= 6.6 (concentrations ranging from 0 to 1000 mg/L). The mixture was stirred at 200 r/min at room temperature until the equilibrium was established in a water shaker bath. Then, the mixture was centrifuged in order to analyze the residual concentration of the CR using a UV-visible spectrophotometer (UV2300II) at λ_{max}=498 nm (Figure 1). All the experiments were conducted in triplicate to ensure the reproducibility of the experience. The adsorbed amounts of CR per gram of ND (mg/g) at equilibrium (q_e) and at a different time (q_t) were calculated as follows:

$$q_{e,t} = \frac{(C_i - C_{e,t})V}{m} \quad (1)$$

The removal percentage (P_R) values were calculated using the following equation:

$$P_R = \frac{C_i - C_{e,t}}{C_i} \times 100\% \quad (2)$$

where C_i (mg/L) and $C_{e,t}$ (mg/L) are the CR concentrations at the beginning, at equilibrium and specific time, respectively. m is the ND mass (g), and V is the total volume of liquid (L).

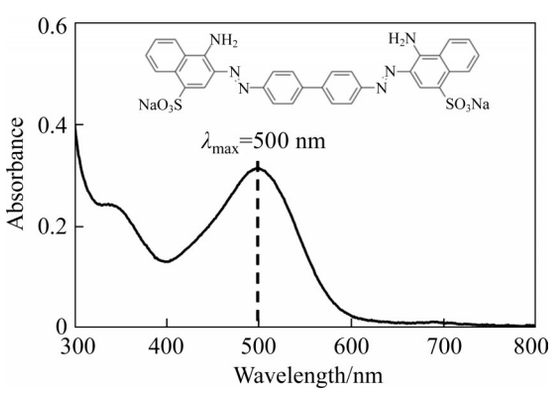

Figure 1 UV-visible spectrum of CR (CR concentration 4.6 mg/L)

The influence of operating conditions such as pH, contact time, adsorbent mass, initial concentration and temperature on the adsorption of CR onto ND was studied in a batch system.

The effect of pH conditions on CR adsorption was conducted by varying the pH of the CR solution (50 mg/L) from 2.0 to 12 at 25 °C. The initial pH was adjusted by adding HCl (0.1 mol/L) or NaOH (0.1 mol/L). The effect of the ND dose on the adsorption of CR was achieved by mixing different mass of ND with a fixed concentration of CR solution (200 mg/L). To investigate the effect of initial CR concentration, 0.1 g of ND was mixed with 50 mL of CR solutions with concentrations ranging between 0 to 500 mg/L at 25 °C without pH adjustment. The effect of temperature on CR adsorption was studied at three different temperatures of 25 °C, 35 °C and 45 °C.

In order to investigate the regeneration of the ND after adsorption, the batch experiments were performed using the following eluting solvents, HCl, NaOH, ethanol, HNO_3 at different concentrations (0−0.5 mol/L): First, a mass (1 g) of ND was loaded with 100 mg/L of CR solution without adjustment and the solution was stirred for 24 h until equilibrium was reached. Upon equilibrium, the ND samples loaded by CR were separated and washed with distilled water to remove any unadsorbed dye; then, the CR-ND was dried at 80 °C for 12 h. The ND sample weighed and placed in contact with the eluting solvent under the same experimental conditions and the amount of desorbed CR dye was quantified using UV-visible spectrophotometry.

The desorption rate (D) was calculated as follows:

$$D = \frac{q_{des}}{q_{ads}} \times 100\% \quad (3)$$

where q_{des} is the amount of adsorbate removed and q_{ads} is the amount initially adsorbed of CR on the ND.

The regeneration of ND sample was studied and five cycles of adsorption and desorption were repeated.

2.3 Column adsorption

In order to assess the effectiveness of ND for continuous mode CR dye adsorption, fixed-bed column experiments were performed.

Adsorption experiments under continuous flow were conducted in a fixed-bed column in Pyrex with 30 cm length and 1.2 cm internal diameter having a volume of ~34 mL (Figure 2). The column was packed with a mass of ND adsorbent and the solution with a known concentration of CR was pumped into the column in a down-flow mode with a peristaltic pump at the desired flow rate (5 ml/L).

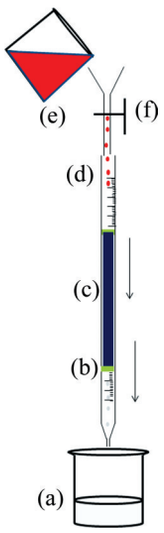

Figure 2 Schematic diagram for fixed-bed column: (a) Collector; (b) Glass wool; (c) ND adsorbent; (d) Column; (e) CR solution tank; (f) Control valve

Glass wool was placed at the bottom to retain the adsorbent as well as at the top of the adsorption column to better distribute the solution onto the medium surface. Small glass beads were used to disperse the ND particles and avoid their agglomeration.

Adsorption characteristics of CR onto ND adsorbent in the fixed-bed column were studied by varying the influent dye concentration (6, 32 and 50 mg/L of CR) and adsorbent mass (0.114, 0.228, 0.342, 0.456 and 0.684 g) with a flow rate of 5 mL/min. The experiments were carried out at room temperature without any pH adjustment.

The treated samples were collected from the bottom of the column at different intervals of adsorption time and the concentration of CR (C_t) in the effluent was measured using a UV-visible spectrophotometer at 498 nm.

Breakthrough curves were obtained by plotting C_{out}/C_{in} (mg/L) against t (min) where C_{out} is the effluent dye concentration, C_{in} is the influent dye concentration and t is the time. All of the experiments were carried out at 25 °C.

3 Results and discussion

3.1 Adsorption kinetics

The equilibrium must be studied to determine the time required to reach equilibrium and to elucidate the mechanism of the adsorption process. The adsorption rate of CR on the ND sample was studied by measuring the amount adsorbed as a function of time, for a constant volume (V=250 mL) and constant initial concentration (C_0=100 mg/L). The ND dose used in the study is 3 g/L. Modeling the results of adsorption kinetics is useful in approaching the mechanism of adsorption of pollutants on solid surfaces. In order to examine the kinetic experimental data and to interpret the adsorption behavior, pseudo-first order and pseudo-second order kinetic models were applied and analyzed based on the regression coefficient (R^2).

The pseudo-first order is given by the expression of Lagergren with the following equation [17]:

$$q_t = q_e(1 - e^{-k_1 t}) \tag{4}$$

While the equation corresponding to the pseudo-second order [18] is expressed as follows:

$$q_t = \frac{k_2 q_e^2 t}{1 + k_2 q_e t} \tag{5}$$

where t is the contact time (min); q_e and q_t are the adsorbed amounts (mg/g) of CR onto ND adsorbent at equilibrium and specific contact time of adsorption, respectively; k_1 (min^{-1}) and k_2 (g/(mg·min)) are the adsorption rate constant related to pseudo-first and pseudo-second-order, respectively.

Figure 3 illustrates the kinetics of CR adsorption onto ND adsorbent. The results indicate rapid initial adsorption of the solute within the first few minutes (0−90 min) with a CR removal rate in the order of 85% which could be attributed to the availability of vacant sites easily accessible in the first minutes, most likely on the external surface of the adsorbent, followed by molecular diffusion of the dye toward less accessible adsorption sites like the interfoliar spaces of the clays, before reaching the adsorption equilibrium [18−19]. Therefore, the adsorption capacity slowly increases over time, until that equilibrium is reached after 90 min and it remains almost stable after 180 min. Hence, the decrease in the adsorption rate could be also explained by the possible formation of monolayers on the surface of the adsorbent [20].

Therefore, we retained 3 h as the time needed to reach CR adsorption equilibrium.

In addition, the fitting of kinetic data to the

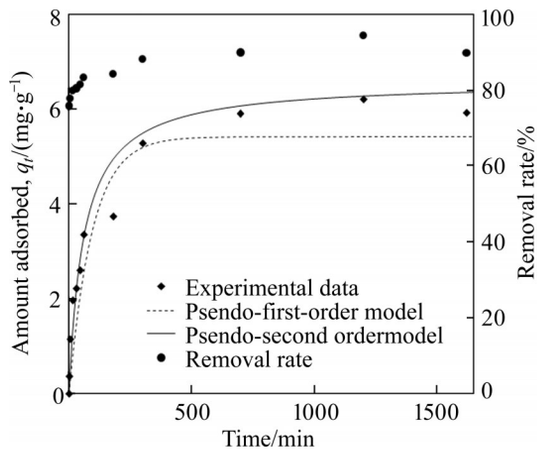

Figure 3 Effect of contact time on the adsorption of CR initial CR concentration: 25 mg/L; ND dose: 3 g/L; temperature: 25 °C; agitation speed: 200 r/min)

pseudo-first and pseudo-second-order models was illustrated, where the goodness of models' fitting to the experimental data is based on the coefficient of determination (R^2) values. The parameters' values related to both models are summarized in Table 2, indicating that the pseudo-second-order model describes the experimental data better than pseudo-first-order (R^2=0.99), which suggests that the chemisorption process behavior is favorable through sharing or exchanging of electrons between CR and ND [21−24].

Table 2 Parameters of kinetic models for adsorption of CR onto ND mineral

Model	Parameter	Value
Kinetic model	q_{exp}/(mg·g^{-1})	5.91
Pseudo-first-order model	q_e/(mg·g^{-1})	5.42
	k_1/min^{-1}	0.01
	R^2	0.91
Pseudo-second-order model	q_e/(mg·g^{-1})	6.59
	k_2/(g·mg^{-1}·min^{-1})	0.01
	R^2	0.99

The adsorption process is significantly influenced by the pH of the solution. The pH of the solution has direct effects on the functional groups present on the surface of adsorbents.

Figure 4 presents the evolution of the adsorbed amount of CR onto ND according to the initial pH values. The effect of pH on the adsorption of CR was investigated by varying the initial pH of the solution from 2 to 12 at 25 °C. The initial solution pH was adjusted by the addition of 0.1 mol/L HCl or 0.1 mol/L NaOH. The amount of ND dose, initial CR concentration and temperature were fixed at 3 g/L, 30 mg/L, and 25 °C, respectively.

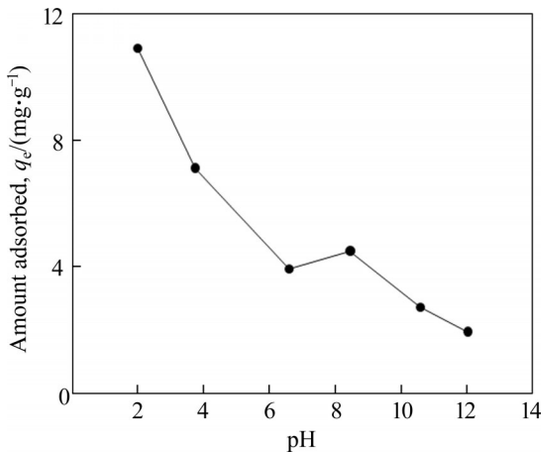

Figure 4 Effect of pH on adsorption of CR onto ND (initial CR concentration: 30 mg/L; diatomite dose: 3 g/L; contact time: 3 h; agitation speed: 200 r/min; temperature: 25 °C)

The results obtained show that the pH strongly affected the adsorption efficiency of CR onto the ND, especially at pH<pH$_{pzc}$ (pH$_{pzc}$=6.5) [11]. The adsorption interactions between active surface sites and CR molecules are obviously pH dependent.

The maximum removal rate of CR takes place at acidic pH (pH=2) with the highest adsorbed amount of 11 mg/g and decreases from 11 to 4 mg/g with increasing pH from 2 to 6. This may be due to the fact that at pH<pH$_{pzc}$, ND surface hydroxyl groups in their protonated form ($X-OH+H^+ \rightarrow X-OH_2^+$) with (X=Si or Al) [25] enhance electrostatic attractions forces with the sulfonate groups of the CR dye. However, at pH>pH$_{pzc}$, ND surface becomes negatively charged ($X-OH+OH^- \rightarrow X-O^- + H_2O$) [26−27], leading to a diminution in the adsorption capacity toward ND. The repulsion forces between the negative charges of ND surface ($X-O^-$) and CR molecules could be responsible for such results [28].

3.2 Adsorbent dose effect

To determine the influence of the ND adsorbent on CR adsorption, the ND dosage was evaluated from 5 to 50 mg/L with a fixed concentration of CR solution (100 mg/L), at room

temperature for a pH 6. Figure 5 indicates that the CR removal efficiency increases rapidly from 12% to 92% as the adsorbent dosage increases. This result can be attributed to the increase of the adsorbent surface area and the high availability of active adsorption sites [29]. The dye removal raised rapidly with the adsorbent dosage increasing until it reached 92% using ND dose of 40 g/L (0.8 g of ND/0.02 L of dye solution), which can be explained by the increase of the surface area and the number of the active sites available on the adsorbent surface. However, a further ND amount did not show a significant change in dye removal because of the susceptible aggregation of adsorption sites or of the split in the concentration gradient that may take place between the solute concentration in the solution and the solute concentration in the surface of the adsorbent [30−32]. It can be also observed that under the conditions studied, the maximum adsorption capacity of CR onto ND is reached (q_e= 6.4 mg/g with 0.3 g of ND).

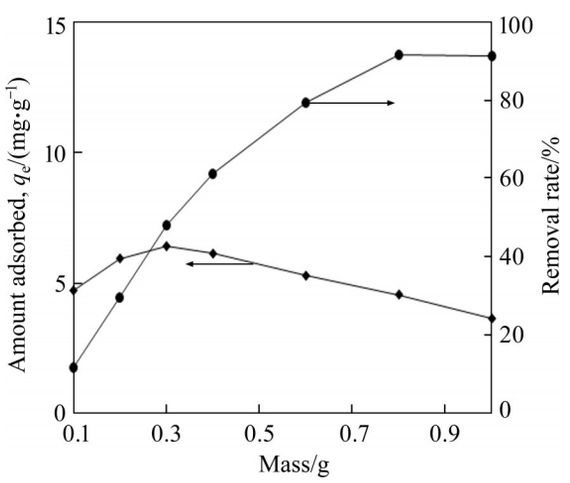

Figure 5 Effect of adsorbent dose on CR removal (pH: 6; initial RC concentration: 100 mg/L; ND amount: 0.1−1.0 g; contact time: 3 h; agitation speed: 200 r/min; temperature: 25 °C)

Hence, the optimal mass of the ND was fixed at 15 g/L with a CR removal of 38% and an adsorbed amount of 6.4 mg/g. This dosage will be used for the next adsorption tests.

3.3 Equilibrium isotherms

The effect of initial concentration on dye adsorption was studied at three temperatures (25 °C, 35 °C and 45 °C) using the same solid-liquid ratio (15 g/L). The initial dye concentrations were varied between 5 mg/L and 500 mg/L. The collected samples were centrifuged for 10 min at a speed of 5000 r/min, then they were analyzed with a UV-visible spectrophotometer. All experiments were performed three times.

3.3.1 Langmuir and Freundlich models (25 °C)

The experimental adsorption data were modeled by Langmuir and Freundlich models [33−34]. The Langmuir adsorption isotherm is the most used model for investigating and characterizing the adsorbent-adsorbate affinity during the adsorption of organic molecules in aqueous solution.

At a constant temperature, the adsorbed quantity q_e is related to (a) the maximum adsorption capacity q_m, (b) the equilibrium concentration C_e of the solute and (c) the affinity constant K_L by the following relationship [35−36]:

$$q_e = \frac{q_m K_L C_e}{1 + K_L C_e} \tag{6}$$

where q_e (mg/g) is the adsorbed amount at equilibrium; C_e is the equilibrium concentration of CR dye (mg/L); K_L (L/mg) is the Langmuir equilibrium constant, which is related to the energy of adsorption the affinity of binding sites; q_{max} (mg/g) is the theoretical monolayer capacity.

Freundlich isotherm model is an empirical equation widely used for the practical representation of the adsorption equilibrium and that occurs on heterogeneous surfaces. Freundlich model is expressed as:

$$q_e = K_F C_e^{1/n} \tag{7}$$

where K_F is Freundlich constant related to the adsorption capacity and n is the heterogeneity factor related to the adsorption intensity.

The dimensionless constant of Langmuir isotherm model (equilibrium parameter R_L) for the adsorption process of CR dye was calculated from Eq. (8).

$$R_L = \frac{1}{1 + K_L C_0} \tag{8}$$

where K_L and C_0 are the Langmuir adsorption constant (L/mg) and the initial dye concentration (mg/L), respectively. All the calculated R_L values are higher than zero and lower than unity ($0<R_L<1$), which reflects a favorable adsorption of CR using ND.

Figure 6 represents the adsorption isotherm of CR onto ND mineral at 25 °C. It presents a straightforward relationship between the amount of adsorbed CR per unit mass of ND (q_e) versus equilibrium concentration (C_e). Langmuir and Freundlich adsorption isotherms are used to fit the experimental data.

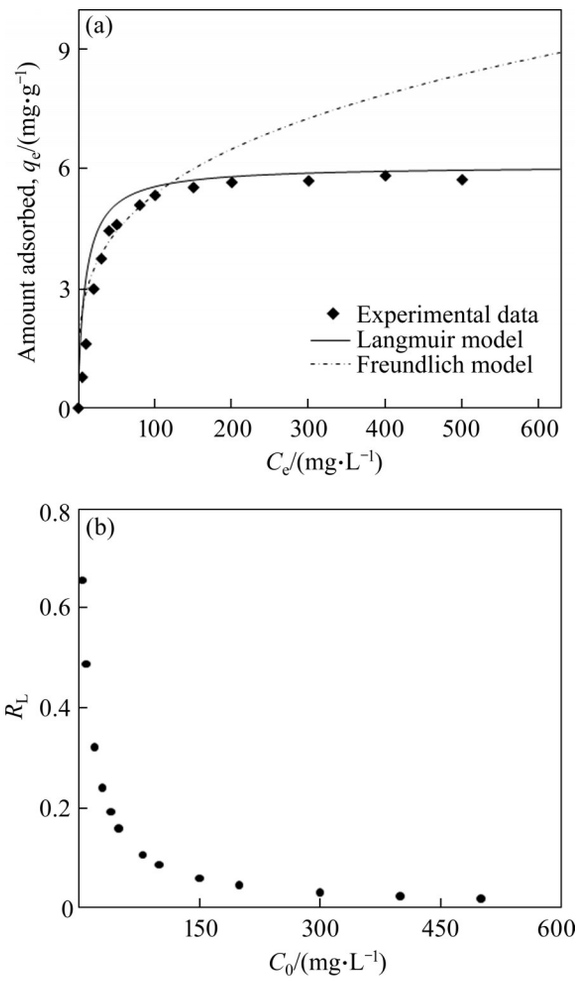

Figure 6 Equilibrium data of CR adsorption onto ND mineral: (a) Model fitting to different adsorption models; (b) Separation factor (R_L) (diatomite amount: 0.3 g; contact time: 3 h, agitation speed: 200 r/min; temperature: 25 °C)

Table 3 summarizes the calculated parameters for the Langmuir and Freundlich isotherms. It was clearly observed that the adsorbed amount given by Langmuir isotherm fitted well the experimental data (R^2=0.97); this was comparable to that obtained from Freundlich isotherm (R^2=0.94).

Due to the higher negative charge present on the ND surface, the adsorbent exhibits a middle affinity and adsorptive capacity for CR due to the repulsion that appears between the ND and CR molecules.

Table 3 Langmuir and Freundlich parameters for CR adsorption onto ND mineral

Model	Isotherm parameter	Value
Langmuir	q_m/(mg·g^{-1})	6.07
	K_L/(L·mg^{-1})	0.11
	R^2	0.97
Freundlich	K_F/(mg·g^{-1})·(L·mg^{-1})	1.49
	n	3.60
	R^2	0.94

In order to show the advantages in the application of ND as a natural mineral for the removal of CR from contaminated waters, the maximum adsorption capacities of CR onto ND are compared with the previously reported data with various low-cost adsorbents [24–26, 37–40] (Table 4). As it can be noticed in the table, the maximum adsorption capacity of CR onto ND is in good agreement with those reported values in the literature for cellulose fiber, cashew net shell, activated carbon, coir pith, and kaolin. However, they are lower than the values reported for cellulose fiber, eucalyptus wood sawdust, cashew net shell, activated carbon, coir pith, kaolin, cone pin and sawdust. Such pieces of evidence support the statement of the feasibility to employ ND as a natural mineral adsorbent for CR removal from

Table 4 The maximum adsorption capacities of different adsorbents used for removal of CR

Adsorbent	Maximum desorption capacity/(mg·g^{-1})	Reference
Diatomite	6.07	Present study
Cellulose fiber	17.39	[37]
Eucalyptus wood sawdust	31.25	[38]
Cashew net shell	5.18	[24]
Activated carbon (LT)	1.88	[25]
Coir pith	6.7	[26]
Kaolin	5.6	[39]
Zeolite	4.3	[39]
Saw dust	5.10	[40]
Cambic chernozem soil (Romanian)	2.24	[41]
Sandy loam, loam and clay Greek soils	0.5–0.625	[42]
Com Cob	50	[43]

aqueous solutions.

3.3.2 Effect of temperature

The temperature has a significant impact on the adsorption process. In fact, the variation of temperature can improve the diffusion of the adsorbate molecules. In general, the modification of temperature changes the equilibrium capacity of the adsorbent [44].

The adsorption isotherms were obtained at different initial concentrations ranging between 25 °C and 45 °C. Results of the effect of temperature on the adsorbed amount of CR onto the ND adsorbent are illustrated in Figure 7. When the temperature of the solution increased from 25 °C to 45 °C, the adsorption capacity of ND decreased slightly from 5.8 to 5.6 mg/g. These results could be attributed to an increase in the solubility of dye molecules with the rise in temperature, increasing the intraparticle diffusion of CR molecules that leads to higher access to active sites available for dye adsorption.

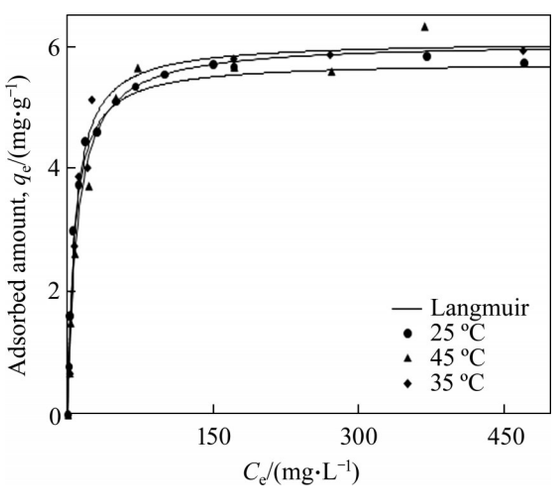

Figure 7 CR adsorption isotherms of ND at different temperatures (diatomite amount: 0.3 g; contact time: 3 h; agitation speed: 200 r/min; temperature: 25 °C−45°C)

3.4 Infrared spectroscopy in transmission mode (FTIR)

The mechanism of the CR adsorption onto ND adsorbent was studied by FTIR technique. FTIR offers some indication about the ability of CR dye to react with functional groups that spread over the surface of ND adsorbent.

Figure 8 shows the FTIR spectra of the ND before and after adsorption of the CR. These spectra were examined for functional groups that contributed to the adsorption process. As seen in Figure 8, the peak at 3400 cm^{-1} is attributed to the stretching vibration of —OH groups. The band at 796 cm^{-1} and 466 cm^{-1} can be attributed to the stretching vibration of the Si—O group in ND and the physically adsorbed water. Shifts or changes to these peaks indicate interactions of the dyes with silanol groups (Si—OH), and can be interpreted as adsorption on neutral sites.

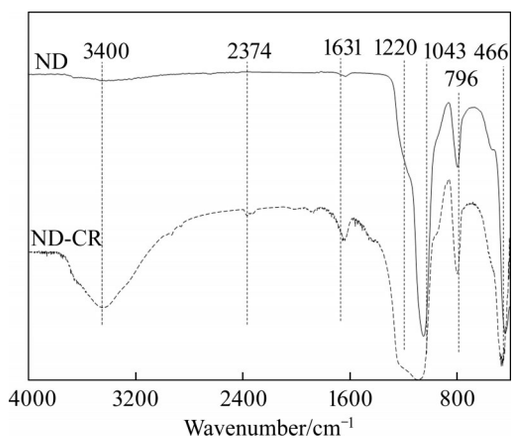

Figure 8 FTIR spectra of ND before and after adsorption of CR

The band of the vibration of the silica group comprising asymmetrical elongation of Si—O—Si is registered at 1043 cm^{-1} [45].

The IR absorption band at 2374 cm^{-1} corresponds to the vibration of the CO_2 elongation mode [46]. In addition, the band around 1634 cm^{-1} could be associated with the mode of deformation of the —OH group [47], while the peak at 1610 cm^{-1} is due to the C—N elongation vibration of the aromatic nucleus of the molecule CR [48].

After adsorption of CR onto ND, a shifting of the clear peak at 796 cm^{-1} (O—H vibration) is observed to 786 cm^{-1}. Similar effects can be observed for the main Si—OH vibration at 3400 cm^{-1}. In addition, the new bands have appeared after adsorption of the CR at 1631 and 1220 cm^{-1}, which are associated with the stretching vibration of the benzene ring [49], suggesting that the adsorption process of CR onto the ND surface was successfully conducted.

3.5 Regeneration

3.5.1 Desorption and ND regeneration

The regeneration of ND adsorbent is an important step in order to check the economic

feasibility of the adsorption process.

The evaluation of desorption was carried out at a temperature of 25 °C, without adjustment and the solution was stirred for 24 h until equilibrium was reached. The concentrations were measured after the desorption step and analyzed by a UV-visible spectrophotometer.

Figure 9 reveals the effects of various chemical products as eluents on desorption efficiency.

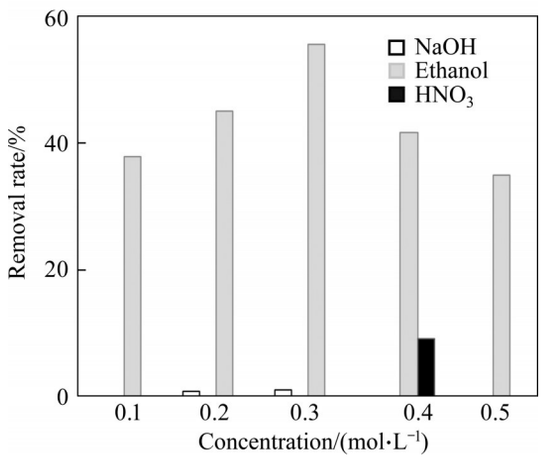

Figure 9 Effect of washing media on the regeneration of ND after adsorption of CR

A very low desorption (~2% or less) was obtained with HCl and NaOH. On the other hand, the desorption step using 0.3 mol/L ethanol was optimum (56%) followed by 0.4 mol/L HNO_3 (10%). The low desorption of CR using HCl and NaOH eluent indicates the formation of chemical bonds between CR and the surface of the ND adsorbent (CR-ND) with the high adsorption heat or the formation of the complexes between the active sites of the ND and the functional groups of CR [50]. The elution efficiency was further investigated at various ethanol concentrations.

3.5.2 Regeneration cycle process

The adsorption/desorption cycles were repeated five times continuously under the same operating conditions as used during the desorption step. The duration of a single adsorption/desorption cycle was 24 h and Figure 10 shows the corresponding cycles of ND encumbered with CR using 0.3 mol/L ethanol.

Regeneration of the ND adsorbent is possible by desorption in 0.3 mol/L ethanol, where the amounts of these eluents can be minimized by at least 50%. The regenerated material can be reused at least twice. As a result, this recycling improves the economic profitability of the natural adsorbent [51].

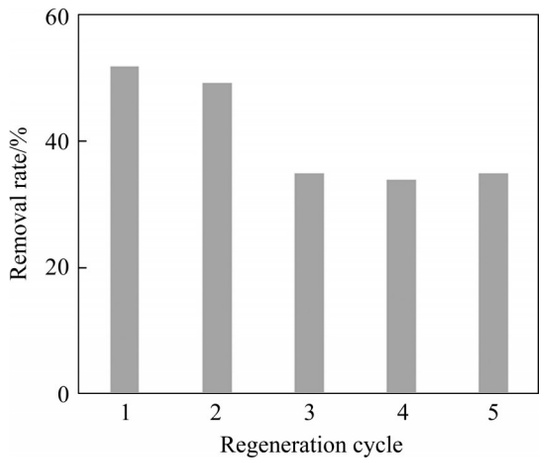

Figure 10 Adsorption/desorption cycles of ND encumbered with CR in a medium of 0.3 mol/L ethanol

3.6 Fixed-bed adsorption

Breakthrough curves for CR adsorption onto the ND adsorbent in continuous flow mode are presented in Figures 11 and 12.

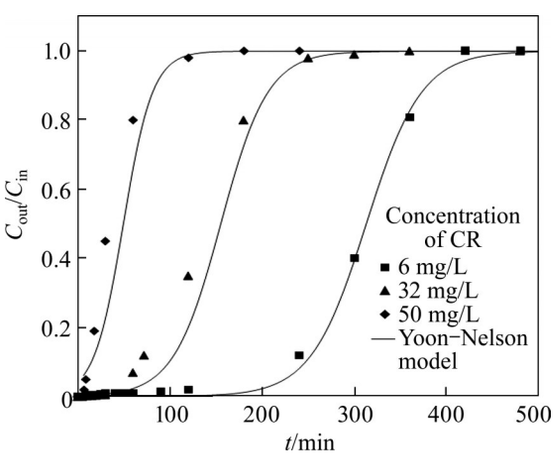

Figure 11 Breakthrough curves at different concentrations of CR dye (Flow rate 1 mL/min, m=0.24 g (bed height=1.1 cm), T=25 °C, without adjustment of pH)

The overall performance of an adsorption column is related to the different parameters as time of breakthrough t_b corresponding to a relative CR concentration C_{out}/C_{in} of 0.05, exhaustion time t_{sat}, adsorption capacity and the removal efficiency.

The adsorption capacity (q_{ads}) was calculated by the equation:

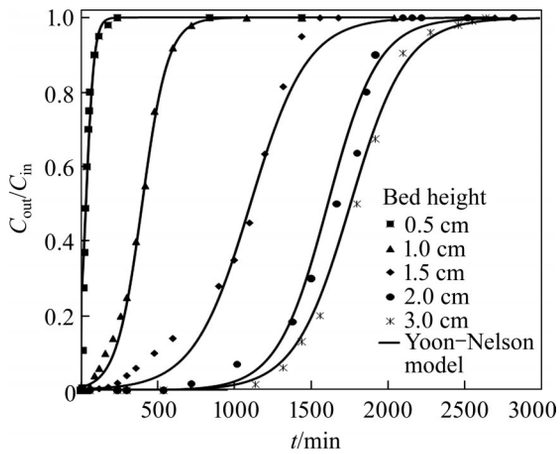

Figure 12 Breakthrough curves at different bed heights (F_{in}=1 mL/min, C_{in}=6 mg/L, T=25 °C, without adjustment of pH)

$$q_{ads}=\frac{F_{in}}{m}\left[(C_{in}\cdot t_a)-\frac{\sum(C_{out_{i+1}}+C_{out\,i})(t_{i+1}-t_i)}{2}\right] \tag{9}$$

where q_{ads} (mg/g) is the adsorbed amount of CR per gram ND; F_{in} (mL/min) is the volumetric flow rate of the solution; C_{in} (mg/L) is the inlet concentration of CR; C_{outi+1} is the outlet concentration at the (i+1)th reading (mg/L); C_{outi} is the outlet concentration at the ith reading (mg/L); t_a is the saturation time; t_{i+1} is the adsorption time at the (i+1)th reading (min); t_i is the adsorption time at the ith reading (min); m (g) is the amount of ND adsorbent.

The effect of influent concentration of CR on the evolution of the ratio C_{out}/C_{in} of CR at the inlet and outlet of the column on ND adsorbent as a function of time is shown in Figure 11 and the obtained parameters are summarized in Table 5.

Table 5 t_b and q_{ads} values at different CR concentrations (C_{out}/C_{in}=0.05, C_{out}/C_{in}=0.5 and C_{out}/C_{in}=1)

C_{in}/(mg·L^{-1})	t_b/min	$t(C_{out}/C_{in}=0.5)$/min	t_{sat}/min	q_{ads}/(mg·g^{-1})
6	230	300	420	5.10
32	50	120	250	6.49
50	9	30	120	6.79

All the breakthrough curves presented the same profile (S-sharpe) characterized by three stages. In the first stage, CR is totally adsorbed. This is mainly due to the filling of the most available porosity where the diffusion rate is fast. In the second stage, the CR concentration gradually reaches the breakthrough point, while the outlet CR concentration increases with the adsorption time, exhibits an S-shaped curve and then attains a plateau corresponding to the adsorption equilibrium.

It is noticed that the breakthrough times at C_{out}/C_{in}=0.05 (noted t_b) decreased with the increase in inlet dye concentration (C_{in}), indicating an early saturation of the ND adsorbent at high concentration levels. It was reached at 230, 50 and 9 min at CR concentrations 6, 32 and 50 mg/L, respectively. At lower influent dye concentrations, flat breakthrough curves were obtained and a breakthrough occurred slower, which means a longer mass transfer zone and lower adsorption rate.

The increase of the CR dye concentration is accompanied by an increase of the total adsorbed amounts (5.10, 6.49 and 6.79 mg/g for 6, 32 and 50 mg/L, respectively). This may be attributed to the improvement in the dye diffusion to the most difficult sites and greater accessibility to the porous surface of the solid.

On the other hand, the model developed by YOON and NELSON [52], was applied to investigate the breakthrough curves behavior of CR on ND adsorbent, according to the following equation:

$$\frac{C_{out}}{C_{in}}=\frac{1}{1+\exp\left[k'(\tau-t)\right]} \tag{10}$$

where C_{in} and C_{out} are the inlet and outlet concentrations of CR, respectively; τ is the time for C_{out}/C_{in}=0.5); k' is a constant that depends on the diffusion characteristics of the mass transfer zone.

The Yoon−Nelson model is based on the assumption that the rate of decrease in the probability of adsorption for each adsorbate molecule is proportional to the probability of adsorbate adsorption and the probability of adsorbate breakthrough on the adsorbent. The Yoon−Nelson model not only is less complicated, but also requires no detailed data concerning the characteristics of adsorbate, the type of adsorbent, and the physical properties of the adsorption column [53−55].

Experiments were conducted to investigate the effect of ND mass on the adsorption capacity of the ND adsorbent. The breakthrough curves obtained for CR adsorption, at different adsorbent masses of 0.114 g (0.5 cm), 0.228 g (1 cm), 0.342 g (1.5 cm),

0.456 g (2 cm) and 0.648 g (3 cm) at a constant flow rate of 1 mL/min and influent CR concentration of 6 mg/L are shown in Figure 12 and the related parameters are reported in Table 6. The results indicate that by increasing the bed height from 0.5 to 3 cm, the CR adsorption capacity of ND increased from 5.71 to 6.08 mg/g.

Table 6 t_b and q_{ads} values at different bed heights (C_{out}/C_{in}= 0.05, C_{out}/C_{in}=0.5 and C_{out}/C_{in}=1)

Bed height/cm	t_b/min	$t(C_{out}/C_{in}=0.5)$/min	t_{sat}/min	q_{ads}/(mg·g^{-1})
0.5	5	30	240	5.71
1	120	390	840	6.02
1.5	360	1104	2040	6.1
2	1020	1668	2520	6.06
3	1320	1800	2640	6.08

Considering C_{out}/C_{in}=0.05, the breakthrough time was 5, 120, 360, 1020 and 1320 min at ND adsorbent masses of 0.114, 0.228, 0.342, 0.456 and 0.648 g, respectively. The saturation time is attained more slowly as adsorbent mass is increased. As the mass increased, CR dye molecules have more time to contact with ND adsorbent, promoting a more efficient removal. The breakthrough curve becomes flatter with the increase in adsorbent mass as a result of the wider solution movement zone. It was found that higher adsorbent mass results in an increase in the adsorption capacity due to a rise in the surface area of the adsorbent which enhances the availability of adsorption sites.

3.7 Proposed mechanism for CR adsorption onto ND

The results of ND characterization obtained by SEM and BET analysis [11] showed that it has a mesoporous structure with irregular and different sizes and shapes. Due to these textural properties, it could be suggested that the adsorption of CR is made not only through the external surface of ND particles, but also through the internal surface of the pores' walls as illustrated in the proposed mechanism of CR adsorption onto ND (Figure 13), offering, therefore, more surface area for chemical reactions and electrostatic interactions between CR molecules and functional groups of ND.

The diatomite surface contains silanol groups that spread over the matrix of the silica. The silanol group is a very active group, which can react with the anionic Congo red and various functional groups. There is an electrostatic (columbic) attraction between CR and the positive charge on the surface of diatomite especially. The analysis of ND indicated that the number of total acidic sites is higher than the basic ones.

The mechanism scheme was suggested according to the textural characteristics and to similar studies [56−60].

4 Conclusions

This work shows the interest of local diatomite mineral as an adsorbent in environmental technology for the treatment of dyes from aqueous

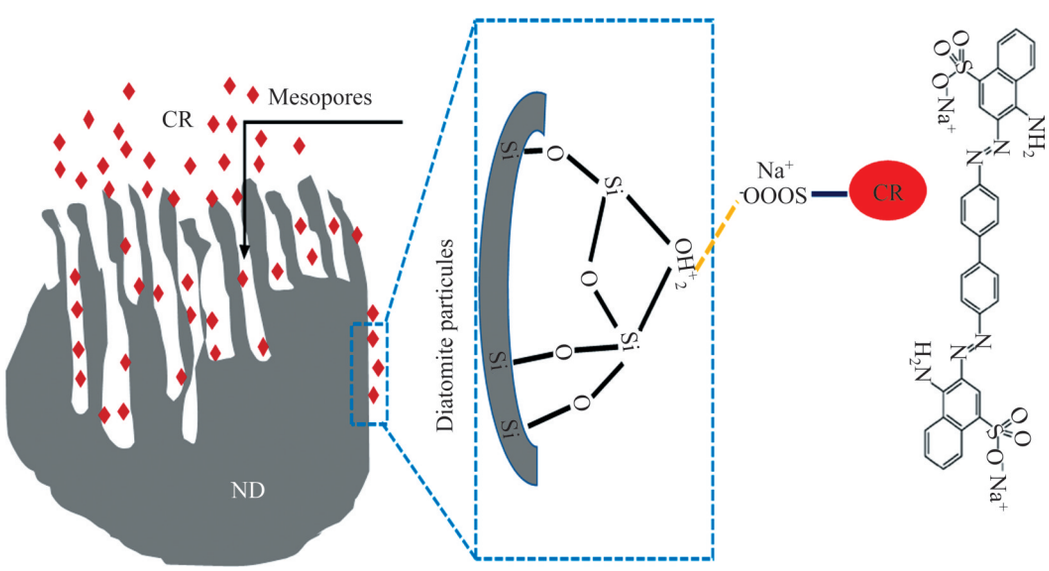

Figure 13 Proposed mechanism of CR adsorption on diatomite surface and possible orientations of CR on the diatomite surface

solutions. The diatomite is abundant and it is really an efficient and economic natural adsorbent of pollutants of dyes compounds.

The adsorptive performances in terms of adsorption and desorption of CR were studied by discontinuous and continuous methods.

Various parameters affecting the adsorption process, including adsorbent dose, solution pH, contact time, initial concentration, and temperature were investigated to evaluate the adsorption of CR onto ND. The results indicate that the adsorption capacity of diatomite is favored in an acidic medium, which leads to the maximum value at pH 2. The electrostatic conditions are thus favorable to the establishment of strong electrostatic attractions between the adsorbate and the adsorbent. The mass effect was significant, and the adsorbed amount increases with the rate of the solid in accordance with the increased availability of active sites.

The kinetic study showed very rapid adsorption and the reaction kinetics have been correlated with the pseudo-second order model.

The monolayer maximum adsorption capacities were found to be 6.07 mg/g for CR onto ND using 15 g/L of ND, pH=6, contact time 3 h. The isotherm study demonstrated that the Langmuir isotherm model gives the best representation of CR dye adsorption equilibrium.

The effectiveness of the different eluent families was evaluated with respect to the desorption of dyes. At least 50% desorption in the case of ethanol/(ND-RC) was achieved. Knowing the optimal concentrations made it possible to tackle the regeneration tests. The conditions adopted showed that the regeneration of the diatomite is indeed possible. The increase in the concentration of dyes and the mass of the ND adsorbent is accompanied by a variation in the values of the total adsorbed amounts. This shows that the process of adsorption of dyes onto diatomite in continuous flow system is related to column height and dye concentration.

Hence, the use of the diatomite as a natural adsorbent in the treatment of industrial effluents seems to be very promising. Nevertheless, we suggest that additional research should be conducted to carry out studies of elaboration of a diatomite-based composite and to elucidate the effect of chemicals and heat treatments of diatomite on their adsorption rate. This work is currently in progress.

Contributors

HADRI Mohamed and HAMDAOUI Mustapha performed the experiments, analyzed and interpreted the data, writing the initial draft of the manuscript. ELMRABET Imane and CHAOUKI Zineb performed the experiments, analyzed and interpreted the data. DRAOUI Khalid analyzed and interpreted the data. DOUHRI Hikmat analyzed and interpreted the data. ZAITAN Hicham supervised, analyzed and interpreted the data, writing review & editing, conceptualization, funding acquisition, resources, validation.

Conflict of interest

The authors declare that they have no conflicts of interest.

References

[1] EL MOSTAFA J. Social and ecological transformation in Morocco and across Africa [R]. Heinrich-Böll-Stiftung-Afrique du Nord, Rabat, 2017.

[2] Business opportunities report for reuse of wastewater in morocco [R]. Commissioned by the Netherlands Enterprise Agency, 2018.

[3] Moroccan climate change policy [R]. Ministry Delegate of the Minister of Energy, Mines, Water and Environment, in charge of Environment, 2014.

[4] MANDIL, OUAZZANI N. Water and wastewater management in Morocco: Biotechnologies application [J]. Sustainable Sanitation Practice, 2013, 1(14): 9−16.

[5] Morocco United Nations Environmental performance reviews [R]. New York and Geneva: United Nations Economic Commission for Europe in Cooperation with United Nations Economic Commission for Africa Office for North Africa. 2014.

[6] OUAZZANI N, BOUHOUM K, MANDI L, et al. Wastewater treatment by stabilization pond: Marrakesh experiment [J]. Water Science and Technology, 1995, 31(12): 75−80. DOI: 10.2166/wst.1995.0462.

[7] Ninth project of drinkable water and sanitation: Evaluation report established by the African bank of development [R]. Kingdom of Morocco, African Development Bank, 2006.

[8] MAKHOKH M, BOURZIZA M. Country report for the expert consultation on wastewater management-Morocco-SEEE-ONEP [R]. Dubai, UAE, 2011.

[9] The World Bank Managing Urban, International Bank for Reconstruction and Development Water scarcity in Morocco annexes to Sections 2 to 4 [R]. 2017.

[10] POLLARD S J T, FOWLER G D, SOLLARS C J, et al. Low-cost adsorbents for waste and waste-water treatment: A review [J]. Science of the Total Environment, 1992,

116(1−2): 31−52. DOI: 10.1016/0048-9697(92)90363-W

[11] HADRI M, CHAOUKI Z, DRAOUI K, et al. Adsorption of a cationic dye from aqueous solution using low-cost Moroccan diatomite: Adsorption equilibrium, kinetic and thermodynamic studies [J]. Desalination and Water Treatment, 2017, 75: 213 − 224. DOI: 10.5004/dwt.2017.20553.

[12] MANE V S, VIJAY BABU P V. Kinetic and equilibrium studies on the removal of Congo red from aqueous solution using Eucalyptus wood (Eucalyptus globulus) saw dust [J]. Journal of the Taiwan Institute of Chemical Engineers, 2013, 44(1): 81−88. DOI: 10.1016/j.jtice.2012.09.013.

[13] SAHA P D, CHAKRABORTY S, CHOWDHURY S. Batch and continuous (fixed-bed column) biosorption of crystal violet by Artocarpus heterophyllus (jackfruit) leaf powder [J]. Colloids and Surfaces B: Biointerfaces, 2012, 92: 262 − 270. DOI: 10.1016/j.colsurfb.2011.11.057.

[14] KAUR S, RANI S, KUMAR V, et al. Synthesis, characterization and adsorptive application of ferrocene based mesoporous material for hazardous dye Congo red [J]. Journal of Industrial and Engineering Chemistry, 2015, 26: 234−242. DOI: 10.1016/j.jiec.2014.11.035.

[15] DICHIARA A B, WEINSTEIN S J, ROGERS R E. On the choice of batch or fixed bed adsorption processes for wastewater treatment [J]. Industrial & Engineering Chemistry Research, 2015, 54(34): 8579 − 8586. DOI: 10.1021/acs.iecr.5b02350.

[16] BHARATHI K S, RAMESH S T. Removal of dyes using agricultural waste as low-cost adsorbents: A review [J]. Applied Water Science, 2013, 3(4): 773−790. DOI: 10.1007/s13201-013-0117-y.

[17] LAGERGREN S K. About the theory of so-called adsorption of soluble substances [J]. Sven Vetenskapsakad Handingarl, 1898, 24: 1−39.

[18] OUSSALAH A, BOUKERROUI A, AICHOUR A, et al. Cationic and anionic dyes removal by low-cost hybrid alginate/natural bentonite composite beads: Adsorption and reusability studies [J]. International Journal of Biological Macromolecules, 2019, 124: 854 − 862. DOI: 10.1016/j.ijbiomac.2018.11.197.

[19] LARGO F, HAOUNATI R, AKHOUAIRI S, et al. Adsorptive removal of both cationic and anionic dyes by using sepiolite clay mineral as adsorbent: Experimental and molecular dynamic simulation studies [J]. Journal of Molecular Liquids, 2020, 318: 114247. DOI: 10.1016/j.molliq.2020.114247.

[20] HO Y S, MCKAY G. Pseudo-second order model for sorption processes [J]. Process Biochemistry, 1999, 34(5): 451−465. DOI: 10.1016/S0032-9592(98)00112-5.

[21] KHALILZADEH SHIRAZI E, METZGER J W, FISCHER K, et al. Removal of textile dyes from single and binary component systems by Persian bentonite and a mixed adsorbent of bentonite/charred dolomite [J]. Colloids and Surfaces A: Physicochemical and Engineering Aspects, 2020, 598: 124807. DOI: 10.1016/j.colsurfa.2020.124807.

[22] WANG Zhong-min, GAO Ming-min, LI Xiao-juan, et al. Efficient adsorption of methylene blue from aqueous solution by graphene oxide modified persimmon tannins [J]. Materials Science and Engineering C, 2020, 108: 110196. DOI: 10.1016/j.msec.2019.110196.

[23] SHAIDA M A, DUTTA R K, SEN A K. Removal of diethyl phthalate via adsorption on mineral rich waste coal modified with chitosan [J]. Journal of Molecular Liquids, 2018, 261: 271−282. DOI: 10.1016/j.molliq.2018.04.031.

[24] SENTHIL KUMAR P, RAMALINGAM S, SENTHAMARAI C, NIRANJANAA M, VIJAYALAKSHMI P, SIVANESAN S. Adsorption of dye from aqueous solution by cashew nut shell: Studies on equilibrium isotherm, kinetics and thermodynamics of interactions [J] Desalination: 2010, 261: 52 − 60. DOI: 10.1016/j.desal.2010.05.032.

[25] AYGÜN A, YENISOY-KARAKAŞ S, DUMAN I. Production of granular activated carbon from fruit stones and nutshells and evaluation of their physical, chemical and adsorption properties [J]. Microporous and Mesoporous Materials, 2003, 66(2−3): 189−195. DOI: 10.1016/j.micromeso.2003.08.028.

[26] NAMASIVAYAM C, KAVITHA D. Removal of Congo red from water by adsorption onto activated carbon prepared from coir pith, an agricultural solid waste [J]. Dyes and Pigments, 2002, 54(1): 47−58. DOI: 10.1016/S0143-7208(02)00025-6.

[27] OSTOLSKA I, WIŚNIEWSKA M. Application of the zeta potential measurements to explanation of colloidal Cr_2O_3 stability mechanism in the presence of the ionic polyamino acids [J]. Colloid and Polymer Science, 2014, 292(10): 2453−2464. DOI: 10.1007/s00396-014-3276-y.

[28] SHAH B A, SHAH A V, MISTRY C B, et al. Surface modified bagasse fly ash zeolites for removal of reactive black-5 [J]. Journal of Dispersion Science and Technology, 2011, 32(9): 1247 − 1255. DOI: 10.1080/01932691.2010.505550.

[29] DE O APOLINÁRIO F, PIRES A P. Oil displacement by multicomponent slug injection: An analytical solution for Langmuir adsorption isotherm [J]. Journal of Petroleum Science and Engineering, 2021, 197: 107939. DOI: 10.1016/j.petrol.2020.107939.

[30] GUPTA V K, JAIN R, SIDDIQUI M N, et al. Equilibrium and thermodynamic studies on the adsorption of the dye rhodamine-B onto mustard cake and activated carbon [J]. Journal of Chemical & Engineering Data, 2010, 55(11): 5225−5229. DOI: 10.1021/je1007857.

[31] NITZSCHE R, GRÖNGRÖFT A, KRAUME M. Separation of lignin from beech wood hydrolysate using polymeric resins and zeolites-Determination and application of adsorption isotherms [J]. Separation and Purification Technology, 2019, 209: 491−502. DOI: 10.1016/j.seppur.2018.07.077.

[32] MESDAGHINIA A, AZARI A, NODEHI R N, et al. Removal of phthalate esters (PAEs) by zeolite/Fe_3O_4: Investigation on the magnetic adsorption separation, catalytic degradation and toxicity bioassay [J]. Journal of Molecular Liquids, 2017, 233: 378 − 390. DOI: 10.1016/j.molliq.2017.02.094.

[33] LANGMUIR I. The adsorption of gases on plane surfaces of glass, mica and platinum [J]. Journal of the American Chemical Society, 1918, 40(9): 1361 − 1403. DOI: 10.1021/ja02242a004.

[34] FREUNDLICH H M F. Over the adsorption in solution [J]. Physical Chemistry, 1906, 57: 385−470. DOI: 10.1515/zpch-1907-5723

[35] HALL K R, EAGLETON L C, ACRIVOS A, et al. Pore- and

solid-diffusion kinetics in fixed-bed adsorption under constant-pattern conditions [J]. Industrial & Engineering Chemistry Fundamentals, 1966, 5(2): 212−223. DOI: 10.1021/i160018a011.

[36] WEBER T W, CHAKRAVORTI R K. Pore and solid diffusion models for fixed-bed adsorbers [J]. AIChE Journal, 1974, 20(2): 228−238. DOI: 10.1002/aic.690200204.

[37] GUPTA V K, PATHANIA D, AGARWAL S, et al. Amputation of Congo red dye from waste water using microwave induced grafted Luffa cylindrica cellulosic fiber [J]. Carbohydrate Polymers, 2014, 111: 556−566. DOI: 10.1016/j.carbpol.2014.04.032.

[38] MANE V S, VIJAY BABU P V. Kinetic and equilibrium studies on the removal of Congo red from aqueous solution using Eucalyptus wood (Eucalyptus globulus) saw dust [J]. Journal of the Taiwan Institute of Chemical Engineers, 2013, 44(1): 81−88. DOI: 10.1016/j.jtice.2012.09.013.

[39] VIMONSES V, LEI Shao-min, JIN Bo, et al. Kinetic study and equilibrium isotherm analysis of Congo Red adsorption by clay materials [J]. Chemical Engineering Journal, 2009, 148(2−3): 354−364. DOI: 10.1016/j.cej.2008.09.009.

[40] ANSARI R, SEYGHALI B, MOHAMMAD-KHAH A, et al. Highly efficient adsorption of anionic dyes from aqueous solutions using sawdust modified by cationic surfactant of cetyltrimethylammonium bromide [J]. Journal of Surfactants and Detergents, 2012, 15(5): 557−565. DOI: 10.1007/s11743-012-1334-3.

[41] PURKAIT M K, MAITI A, DASGUPTA S, et al. Removal of Congo red using activated carbon and its regeneration [J]. Journal of Hazardous Materials, 2007, 145(1−2): 287−295. DOI: 10.1016/j.jhazmat.2006.11.021.

[42] GHAEDI M, BIYAREH M N, KOKHDAN S N, et al. Comparison of the efficiency of palladium and silver nanoparticles loaded on activated carbon and zinc oxide nanorods loaded on activated carbon as new adsorbents for removal of Congo red from aqueous solution: Kinetic and isotherm study [J]. Materials Science and Engineering C, 2012, 32(4): 725−734. DOI: 10.1016/j.msec.2012.01.015.

[43] OJEDOKUN A T, BELLO O S. Liquid phase adsorption of Congo red dye on functionalized corn cobs [J]. Journal of Dispersion Science and Technology, 2017, 38(9): 1285−1294. DOI: 10.1080/01932691.2016.1234384.

[44] ALKAN N, FLUHR R, SHERMAN A, et al. Role of ammonia secretion and pH modulation on pathogenicity of Colletotrichum coccodes on tomato fruit [J]. Molecular Plant-Microbe Interactions: MPMI, 2008, 21(8): 1058−1066. DOI: 10.1094/MPMI-21-8-1058.

[45] MADEJOVÁ J. Baseline studies of the clay minerals society source clays: Infrared methods [J]. Clays and Clay Minerals, 2001, 49(5): 410−432. DOI: 10.1346/ccmn.2001.0490508.

[46] MUNAGAPATI V S, KIM D S. Adsorption of anionic azo dye Congo Red from aqueous solution by Cationic Modified Orange Peel Powder [J]. Journal of Molecular Liquids, 2016, 220: 540−548. DOI: 10.1016/j.molliq.2016.04.119.

[47] SAIKIA B J, PARTHASARATHY G. Fourier transform infrared spectroscopic characterization of kaolinite from Assam and Meghalaya, northeastern India [J]. Journal of Modern Physics, 2010, 1(4): 206−210. DOI: 10.4236/jmp.2010.14031.

[48] RATHEE G, AWASTHI A, SOOD D, et al. A new biocompatible ternary Layered Double Hydroxide Adsorbent for ultrafast removal of anionic organic dyes [J]. Scientific Reports, 2019, 9: 16225. DOI: 10.1038/s41598-019-52849-4.

[49] IMAMURA K, IKEDA E, NAGAYASU T, et al. Adsorption behavior of methylene blue and its congeners on a stainless steel surface [J]. Journal of Colloid and Interface Science, 2002, 245(1): 50−57. DOI: 10.1006/jcis.2001.7967.

[50] MALL I D, SRIVASTAVA V C, KUMAR G V A, et al. Characterization and utilization of mesoporous fertilizer plant waste carbon for adsorptive removal of dyes from aqueous solution [J]. Colloids and Surfaces A: Physicochemical and Engineering Aspects, 2006, 278(1−3): 175−187. DOI: 10.1016/j.colsurfa.2005.12.017.

[51] SHAH I, PRÉ P, ALAPPAT J. B. Steam regeneration of adsorbents: An experimental and technical review [J]. Chemical Science Transactions, 2013, 2(4): 1078−1088. DOI: 10.7598/cst2013.545.

[52] YOON Y H, NELSON J H. Application of gas adsorption kinetics I. A theoretical model for respirator cartridge service life [J]. American Industrial Hygiene Association Journal, 1984, 45(8): 509−516. DOI: 10.1080/15298668491400197.

[53] ZAITAN H, KORRIR A, CHAFIK T, et al. Evaluation of the potential of volatile organic compound (di-methyl benzene) removal using adsorption on natural minerals compared to commercial oxides [J]. Journal of Hazardous Materials, 2013, 262: 365−376. DOI: 10.1016/j.jhazmat.2013.08.071.

[54] HAN Run-ping, WANG Yu, ZHAO Xin, et al. Adsorption of methylene blue by phoenix tree leaf powder in a fixed-bed column: Experiments and prediction of breakthrough curves [J]. Desalination, 2009, 245(1−3): 284−297. DOI: 10.1016/j.desal.2008.07.013.

[55] AKSU Z, GÖNEN F. Biosorption of phenol by immobilized activated sludge in a continuous packed bed: Prediction of breakthrough curves [J]. Process Biochemistry, 2004, 39(5): 599−613. DOI: 10.1016/S0032-9592(03)00132-8.

[56] AL-GHOUTI M A, AL-DEGS Y S, KHRAISHEH M A M, et al. Mechanisms and chemistry of dye adsorption on manganese oxides-modified diatomite [J]. Journal of Environmental Management, 2009, 90(11): 3520−3527. DOI: 10.1016/j.jenvman.2009.06.004.

[57] KHRAISHEH M A M, AL-GHOUTI M A, ALLEN S J, et al. The effect of pH, temperature, and molecular size on the removal of dyes from textile effluent using manganese oxides-modified diatomite [J]. Water Environment Research, 2004, 76(7): 2655−2663.

[58] ZHANG Chun-hui, JIANG Shan, TANG Jia-wei, et al. Adsorptive performance of coal based magnetic activated carbon for perfluorinated compounds from treated landfill leachate effluents [J]. Process Safety and Environmental Protection, 2018, 117: 383−389. DOI: 10.1016/j.psep.2018.05.016.

[59] SILVA V C, ARAÚJO M E B, RODRIGUES A M, et al. Adsorption behavior of acid-treated Brazilian palygorskite for cationic and anionic dyes removal from the water [J]. Sustainability, 2021, 13(7): 3954. DOI: 10.3390/su13073954.

[60] SRIRAM G, KIGGA M, UTHAPPA U T, et al. Naturally available diatomite and their surface modification for the removal of hazardous dye and metal ions: A review [J]. Advances in Colloid and Interface Science, 2020, 282: 102198. DOI: 10.1016/j.cis.2020.102198.

(Edited by HE Yun-bin)

中文导读

天然硅藻土矿物的高值化利用：在批式和固定床反应器中去除水溶液中的阴离子染料

摘要：以摩洛哥硅藻土(ND)为低成本吸附剂，采用批式和柱式吸附法对污染水体中刚果红(CR)染料的去除效率进行研究。考察了实验条件(pH、吸附剂剂量和温度)对ND吸附CR的影响。实验结果表明，在15 g/L ND、pH=6、接触时间为3 h、温度为25 °C的条件下，CR的吸附量为6.07 mg/g，拟二级吸附模型与实验动力学数据吻合较好，Langmuir等温线模型能较好地描述吸附平衡数据。再生实验结果表明，当以乙醇为洗脱剂时，ND的解吸率达到50%。此外，还研究了连续模式下的吸附过程。用Yoon−Nelson模型可以很好地解释穿透曲线。在25 °C条件下，当吸附剂用量为0.114 g，CR浓度为6 mg/L，流量为1 mL/min时，吸附量可达5.71 mg/g。

关键词：刚果红；吸附；硅藻土；固定床柱；动力学模型